

Synthetic Lipidation of Peptides and Amino Acids: Monolayer Structure and Properties

Peter Berndt,^{†,‡} Gregg B. Fields,^{†,§} and Matthew Tirrell^{*,†,‡}

Contribution from the Biomedical Engineering Center, Department of Chemical Engineering and Materials Science, and Department of Laboratory Medicine and Pathology, University of Minnesota, Minneapolis, Minnesota 55455

Received May 26, 1995[⊙]

Abstract: Novel dialkyl chain amphiphiles containing peptides derived from extracellular matrix collagen ligand sequences have been synthesized using a highly efficient solid-phase approach. These compounds have been shown to form stable monolayers at the air–water interface. Monolayer features are determined by the peptide head group and are dependent on the peptide sequence. The peptide packing implied by the head group area is denser than the packing of a fully hydrated random coil structure. At high surface pressures, peptide amphiphiles can be compressed to molecular areas corresponding to fully extended peptide chains. The interfacial monolayer behavior of the peptide amphiphiles is compared to that of a series of novel compounds containing various amino acids in their head group region. Monolayers of these compounds permit investigation of model membranes containing the functional elements of proteins such as those involved in cell adhesion and signaling.

Introduction

One of the important insights of molecular biology obtained in the last few years is the elucidation of a mechanism for the ability of eucaryotic cells to recognize their location in tissue. The mechanism of tissue recognition has been traced to the interaction of a relatively small number of extracellular tissue markers with corresponding receptors at the cell surface. Extracellular markers have a profound influence on cell adhesion and spreading, and in many cases, their presence directs cell growth.^{1–3}

The extracellular markers are often found to be relatively short sequences in the fibrous proteins ubiquitous in extracellular matrices such as collagen and fibronectin. Given the enormous size and variability of these fibrous proteins, it is very challenging to study the molecular mechanism of the interaction between extracellular ligands and cell surface receptors. This interaction must be highly specific, and of substantial strength, with a few hundreds of molecular interactions capable of fixing a whole cell permanently to a surface.

One of the problems of studying extracellular matrix–cell receptor interactions is the creation of an experimental system that enables measurement of the adhesive interaction strength. The ideal experimental system should feature a strictly defined number of recognition sequences in native conformation on a surface large enough to hold cells. With these issues in mind, we have developed a novel model system in which ligand–receptor pairs can be incorporated into separate lipid molecules and fixed via self-assembly onto a highly organized monolayer surface.

This approach to the investigation of ligand–receptor interactions holds many advantages. First, one can examine a given interaction at a fixed, controllable, nonequilibrium separation between the binding molecules. Second, the investigated interaction at the surface is accessible to direct macroscopic

physicochemical methods such as surface forces measurement, X-ray scattering, and infrared spectroscopy. Third, the interaction is at the surface–water phase boundary, that is, under the conditions similar to those *in vivo*. Finally, functionalized mono- and bilayer-forming amphiphiles could be the building blocks for complex self-assembling membrane systems with multiple receptor or catalytic properties (artificial enzymes, targeted drug delivery, biocompatible coatings).⁴ In the present paper, we report an efficient pathway for the synthesis of amphiphiles containing a peptide in their hydrophilic component (head group) and dialkyl or diacyl chains in their hydrophobic components (tails).

Interest in this class of compounds has been rising steadily during the last decade. Early attempts at synthesizing peptide amphiphiles coupled natural lipid tails (i.e., phosphatidylethanolamine) in a solution reaction with relatively short peptides.^{5,6} Solution phase coupling was a necessity before widespread application of Fmoc solid-phase peptide synthesis, since most lipid tail groups would not be stable during deprotection and cleavage in strong mineral acids that are required by Boc chemistry. However, the solution phase approach is plagued by the mutual immiscibility of the hydrophilic and hydrophobic components of the desired molecule, which tends to aggravate problems during head group-to-tail coupling and peptide deprotection. Therefore, we are not surprised that, despite their tremendous potential, peptide amphiphiles have not been widely explored.

Lipidated peptides and proteins⁷ have been found in several crucial regulatory and signal transducing functions in eucaryotic cells^{8–12} and often the lipid modification determines their activity and subcellular location. Most interesting from the point

(4) Ringsdorf, H.; Schlarb, B.; Venzmer, J. *Angew. Chem.* **1988**, *27*, 113–58.

(5) Jain, R. K.; Gupta, C. M.; Anand, N. *Tetrahedron Lett.* **1981**, *22*, 2317–20.

(6) Thompson, N. L.; Brian, A. A.; McConnell, H. M. *Biochim. Biophys. Acta* **1984**, *772*, 10–19.

(7) Casey, P. J. *Science* **1995**, *268*, 221–25.

(8) Carr, C.; Tyler, A. N.; Cohen, J. B. *FEBS Lett.* **1989**, *243*, 65–9.

(9) Busconi, L.; Michel, T. *J. Biol. Chem.* **1993**, *268*, 8410–3.

(10) George, D. J.; Blackshear, P. J. *J. Biol. Chem.* **1992**, *267*, 24879–85.

[†] Biomedical Engineering Center.

[‡] Department of Chemical Engineering and Materials Science.

[§] Department of Laboratory Medicine and Pathology.

[⊙] Abstract published in *Advance ACS Abstracts*, September 1, 1995.

(1) Humphries, M. J. *J. Cell Sci.* **1990**, *97*, 585–592.

(2) Akiyama, S. K.; Yamada, K. M. *Cancer Biol.* **1993**, *4*, 215–28.

(3) Zetter, B. R. *Cancer Biol.* **1993**, *4*, 219–29.

of view of biochemistry are myristoylated peptides as substrates or inhibitors of two important cellular proteins: myristoyl-CoA: protein *N*-myristoyl transferase (which is probably a major target during oncovirus-induced cell transformation)^{13–17} and protein kinase C.^{18–20} For many of these peptides, fully synthetic analogs have been obtained as important research tools.

Due to the stability of aliphatic amides to strong mineral acid treatment, Boc solid-phase synthesis of *N*-myristoylated peptides has been employed extensively. These compounds have primarily been in the focus of biochemical investigation, and thus little is known about their physicochemical and membrane-forming properties. Nevertheless, it has been shown that *N*-myristoylated peptides can form micelles and spontaneously insert into phospholipid membranes.²¹

Whereas *N*-myristoylated peptides have enjoyed significant attention during the last decade, synthesis of membrane-forming compounds with dialkyl or diacyl chain hydrophobic tail groups has rarely been attempted.^{22,23} De Bont *et al.* published the only example known to us of a synthesis of a diacyl glycerol ester based peptide amphiphile solely by solid-phase techniques using pentafluorophenyl esters of the hydrophobic tail.²⁴ However, the amphiphilic and biological properties of these molecules have not been reported.

We have synthesized peptide amphiphiles using the solid-phase approach with a very simple but versatile hydrophobic tail group introduced by Kunitake *et al.*²⁵ The simplicity of this approach facilitates synthesis and potentially allows us to obtain a large variety of peptide amphiphiles necessary for systematic study of their structural and biological properties.

The peptide sequences used in our study are derived from various collagen fragments that have been of considerable interest in the study of tumor cell adhesion and spreading. In the early 1980s it was established that certain tumor cell lines bind extracellular matrix components (including collagen) via specific integrin and proteoglycan receptors on the cell surface.²⁶ This interaction determines cell motility, morphology, and histological appearance to a large extent. In recent years, numerous collagen ligand sequences for cell membrane receptors have been identified and extensively studied. Ligand sequences have been found in different collagen types.^{27–29} Some of these sequences are truly remarkable in their ability to maintain folded

structures in aqueous solution. For example, the $\alpha 1(IV)1263$ – 1277 collagen sequence Gly-Val-Lys-Gly-Asp-Lys-Gly-Asn-Pro-Gly-Trp-Pro-Gly-Ala-Pro (*[IV-H1]*), which promotes tumor cell adhesion,²⁸ has been shown to assume a β -turn-like structure in solution.³⁰ When this sequence is flanked by repeating Gly-Pro-Hyp sequences, circular dichroism data indicates the possibility of triple-helical assembly.³¹ Other sequences, like the hydrophobic collagen fragment $\alpha 1(IV)531$ – 543 Gly-Glu-Phe-Tyr-Phe-Asp-Leu-Arg-Leu-Lys-Gly-Asp-Lys (*[HEP III]*), assume a different but regular solution structure.

We synthesized peptide amphiphiles containing *[IV-H1]* or *[HEP III]* sequences to start detailed investigations on their structure, their interaction with their natural receptors, and their biological activity. To show the flexibility of our synthetic approach, we also report data for a 26-amino acid head group peptide Gly-Val-Lys-Gly-Asp-Lys-Gly-Asn-Pro-Gly-Trp-Pro-Gly-Ala-Pro-Gly-Pro-Hyp-Gly-Pro-Hyp-Gly-Pro-Gly-Pro-Hyp that combines the *[IV-H1]* sequence with a triple-helical repeating sequence. In order to be able to differentiate between features induced by the hydrophobic tail portion of the molecule and the hydrophilic peptide head group, we decided to synthesize a number of amphiphile molecules that contain the same tail region as our peptide amphiphiles, but only a single amino acid residue in the head group. As shown below, these molecules also prove very useful for the study of single amino acid side chain interactions. Amphiphiles containing single amino acids were synthesized using classical solution phase chemistry methods with OBz-protected amino acids and *p*-nitrophenyl esters, thus demonstrating yet another facile synthesis scheme suitable for obtaining peptide and/or amino acid lipids.

Results and Discussion

Synthesis of a Hydrophobic Tail Compound. The target compound for a prospective tail has to satisfy certain conditions. The compound should contain two alkyl chains, it should be easy to synthesize and to purify, and in order to be useful in biomedical applications, it should be similar (biocompatible) but not identical (resistant to degrading enzymes) to biological lipids. We evaluated several different compounds (i.e., dialkylamines, phospholipids) for our purposes. Dialkyl glutamates satisfy the above criteria best.

Synthesis of (C₁₆)₂-Glu-C₂-pNp is depicted in Figure 1. The dialkyl ester of Glu was readily obtained by acid-catalyzed condensation of Glu with the appropriate fatty acid alcohol. The *p*-toluenesulfonate salt of Glu dialkyl ester crystallized easily; therefore, extensive purification was conducted at this step. The synthesis of the hydrophobic backbone was followed by succinylation of the free amino group and subsequent activation of the carboxylic acid with *p*-nitrophenol and dicyclohexylcarbodiimide. As both reactions have virtually 100% yields, losses occur only during the necessary purification steps. The whole synthesis can be completed in less than 1 week. The resulting pNp-ester is stable for extensive time periods.

Whereas one might argue that dialkylamides of Glu²³ could have potential advantages, such as excellent stability in strong mineral acids, we found that the poor solubility of these compounds is a serious obstacle for their use in solid-phase synthesis of peptide amphiphiles.

Synthesis of Amphiphiles with Peptide Head Groups. We treat the synthesis of peptide amphiphiles as an extension of

(11) Deichaite, I.; Casson, L. P.; Ling, H. P.; Resh, M. D. *Mol. Cell. Biol.* **1988**, *8*, 4295–701.

(12) Martin, I.; Haro, I.; Reig, F.; Alsina, M. A. *Langmuir* **1994**, *10*, 784–9.

(13) Heuckeroth, R. O.; Jackson-Machelski, E.; Adams, S. P.; Kishore, N. S.; Huhn, M.; Katoh, A.; Lu, T.; Gokel, G. W.; Gordon, J. I. *J. Lipid Res.* **1990**, *31*, 1121–9.

(14) Heuckeroth, R. O.; Towler, D. A.; Adams, S. P.; Glaser, L.; Gordon, J. I. *J. Biol. Chem.* **1988**, *263*, 2127–33.

(15) Kishore, N. S.; Wood, D. C.; Mehta, P. P.; Wade, A. C.; Lu, T.; Gokel, G. W.; Gordon, J. I. *J. Biol. Chem.* **1993**, *268*, 4889–902.

(16) Paige, L. A.; Zheng, G. Q.; DeFrees, S. A.; Cassidy, J. M.; Geahlen, R. L. *Biochemistry* **1990**, *29*, 10566–73.

(17) Zheng, G. Q.; Hu, X.; Cassidy, J. M.; Paige, L. A.; Geahlen, R. L. *J. Pharm. Sci.* **1994**, *83*, 233–8.

(18) Verghese, G. M.; Johnson, J. D.; Vasulka, C.; Haupt, D. M.; Stumpo, D. J.; Blackshear, P. J. *J. Biol. Chem.* **1994**, *269*, 9361–7.

(19) Ward, N. E.; O'Brian, C. A. *Biochemistry* **1993**, *32*, 11903–9.

(20) McIlroy, B. K.; Walters, J. D.; Blackshear, P. J.; Johnson, J. D. *J. Biol. Chem.* **1991**, *266*, 4959–64.

(21) Sankaram, M. B. *Biophys. J.* **1994**, *67*, 105–12.

(22) Prass, W.; Ringsdorf, H.; Bessler, W.; Wiesmueller, K. H.; Jung, G. *Biochim. Biophys. Acta* **1987**, *900*, 116–28.

(23) Shimizu, T.; Hato, M. *Biochim. Biophys. Acta* **1993**, *1147*, 50–58.

(24) De Bont, H. B. A.; Van Boom, J. H.; Liskamp, R. M. J. *Recl. Trav. Chim. Pays-Bas* **1992**, *111*, 222–6.

(25) Asakuma, S.; Okada, H.; Kunitake, T. *J. Am. Chem. Soc.* **1991**, *113*, 1749–55.

(26) Ruoslahti, E.; Engvall, E. *Biochim. Biophys. Acta* **1980**, *631*, 350–8.

(27) Faassen, A. E.; Schragar, J. A.; Klein, D. J.; Oegema, T. R.; Couchman, J. R.; McCarthy, J. B. *J. Cell Biol.* **1992**, *116*, 521–31.

(28) Chelberg, M. K.; McCarthy, J. B.; Skubitz, A. P. N.; Furcht, L. T.; Tsilibary, E. C. *J. Cell Biol.* **1990**, *111*, 261–70.

(29) LeBaron, R. G.; Hook, A.; Esko, J. D.; Gay, S.; Hook, M. *J. Biol. Chem.* **1989**, *264*, 7950–6.

(30) Daragan, V. A.; Ilyina, E.; Mayo, K. H. *Biopolymers* **1993**, *33*, 521–33.

(31) Fields, C. G.; Mickelson, D. J.; Drake, S. L.; McCarthy, J. B.; Fields, G. B. *J. Biol. Chem.* **1993**, *268*, 14153–60.

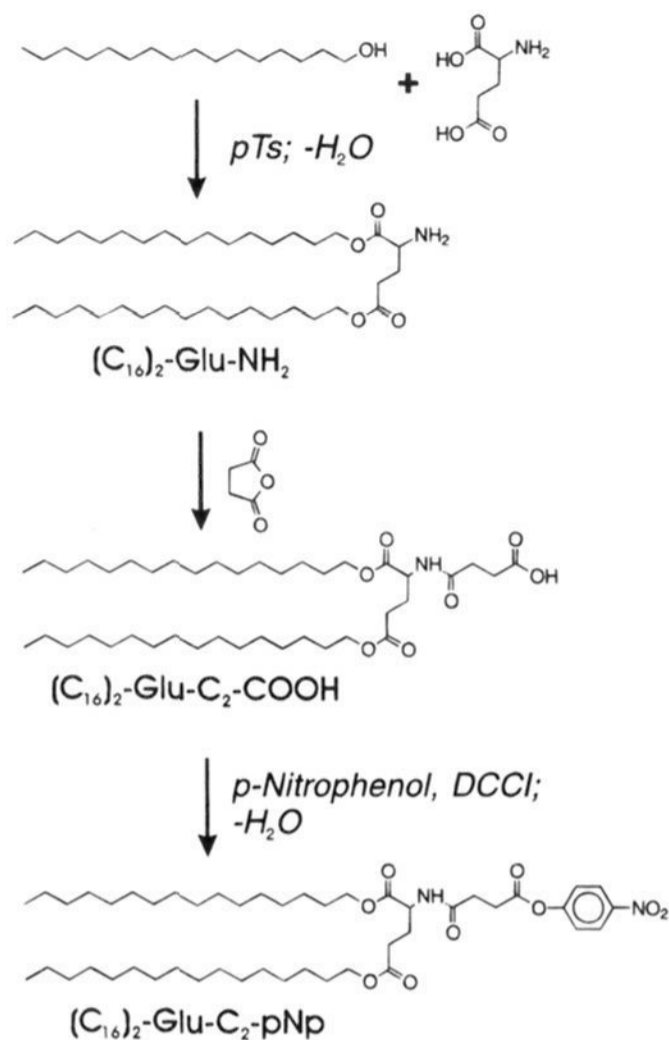


Figure 1. Chemical synthesis of activated tail compound $(C_{16})_2\text{-Glu-C}_2\text{-pNp}$. Condensation between a long-chain alcohol and Glu is achieved by acid catalysis and constant water removal. The resulting Glu ester is succinylated, and the free carboxy group is activated with *p*-nitrophenol.

solid-phase chemistry. This logic demands synthesis of a fully protected peptide head group precursor separately from the tail. The lipophilic tail compound can then be linked to the peptide head group on resin, either as an activated compound (*p*-nitrophenyl ester) or via traditional carbodiimide–hydroxybenzotriazole reaction that forms an active ester *in situ*. TFA-labile resins and Fmoc chemistry allow for easy deprotection, isolation, and purification of the desired compound.

Peptides were synthesized by Fmoc methodology using commercially available Rink resin.³² After coupling of the last amino acid, a small portion of the peptide was deprotected, cleaved, and analyzed by HPLC, mass spectrometry, and Edman degradation sequence analysis. In this way, we assured that the amino acid sequence in the amphiphile was correct. After removal of the N-terminal Fmoc group with 20% piperidine in DMF, the tail compound was coupled to the protected peptide on the resin (Figure 2) in dichloromethane/dimethylformamide for 4 h. After deprotection and cleavage from the resin by 95% trifluoroacetic acid in presence of appropriate scavengers,³³ the peptide amphiphile was precipitated with cold ether, dried, and purified by HPLC using a C_4 reversed-phase column (Figure 3). We note that the only major impurity found in the crude precipitate was *unmodified peptide*. After purification, peptide amphiphiles run as a single peak (>98% purity) on an analytical HPLC column.

The final compounds were characterized by mass spectrometry and NMR (Figure 4). Whereas it is not necessary to identify all correlations present in the complex NMR spectrum, we would like to point out to the presence of alkyl methylenes (cross peak at δ_H 1.48– δ_C 27.0), the signature of an alkyl ester (δ_H 4.0– δ_C 47.0), and the signature of the five protons bound

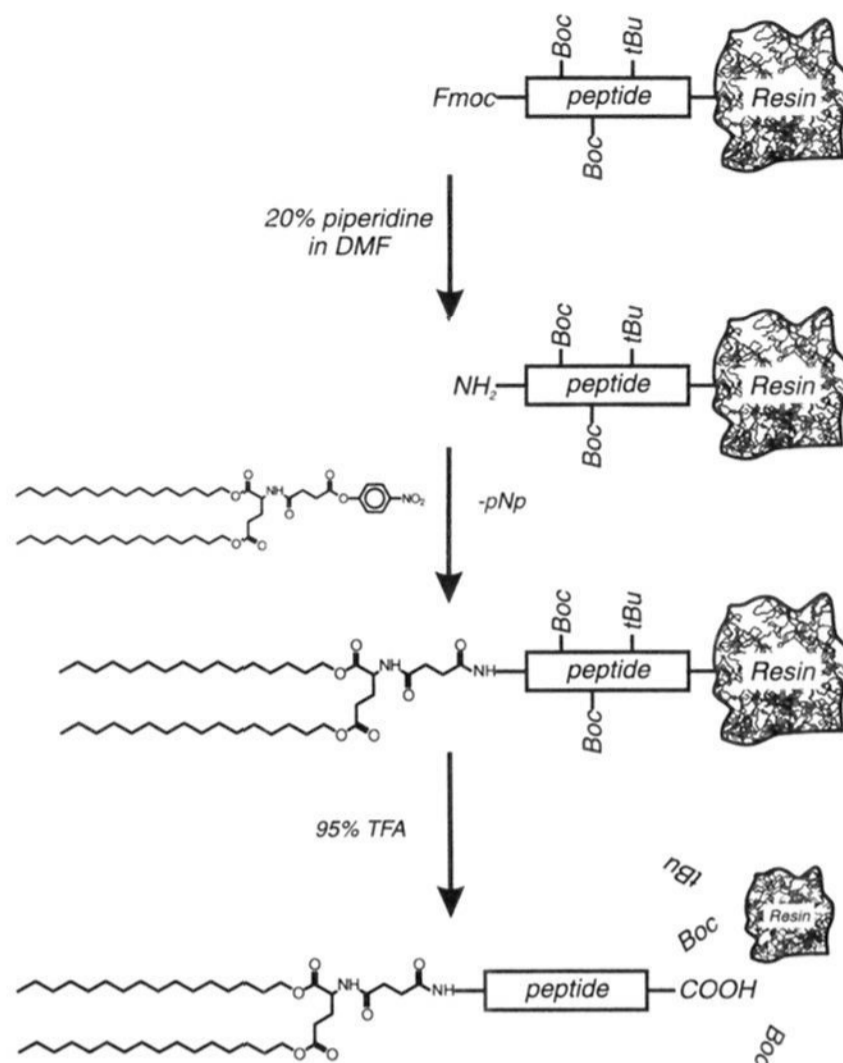


Figure 2. Synthesis of peptide amphiphiles by an extension of solid-phase Fmoc technique. A protected peptide is synthesized on a conventional peptide synthesizer, the amine-protecting Fmoc group is removed with piperidine, and the activated lipophilic tail compound is added. After completion of the synthesis, the peptide amphiphile is deprotected and cleaved from the resin by mild acid treatment.

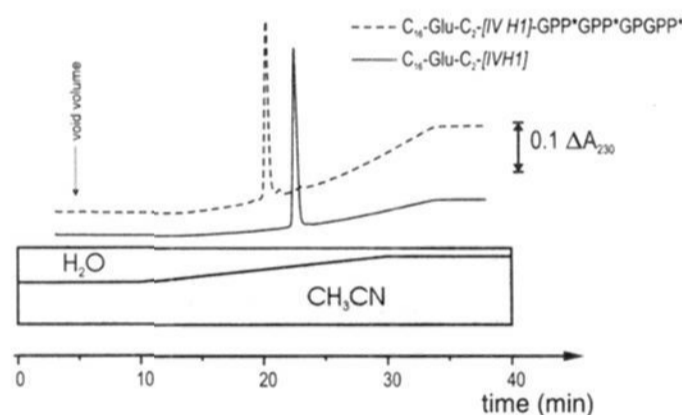


Figure 3. HPLC of peptide amphiphiles. All traces were recorded by eluting the sample with a 55–90% acetonitrile in a water (0.05% TFA) gradient from a Vydac C_4 column.

to the Trp present in the peptide sequence. Further characterization details are given in the Experimental Section.

Using mass spectrometry, we could not find hydrolysis products of the Glu ester; therefore, we conclude that the tail compound is stable under the mild acid treatment used for deprotection and cleaving of the peptide.

Synthesis of Amphiphiles with Amino Acid Head Groups. The solid-phase methodology described above is very well suited to the synthesis of peptide amphiphiles in quantities of up to 100 mg, whereas synthesis of larger amounts (grams) of simple amino acid amphiphiles is possible, but clearly not economical. Therefore, we decided to develop a simple liquid phase procedure for the latter goal (Figure 5).

$(C_{16})_2\text{-Glu-C}_2\text{-pNp}$ readily reacts with primary amines, including amino acid OBz esters, in presence of triethylamine. The removal of the protecting group is easily achieved using catalytic hydrogenation in presence of palladium on charcoal, and the final compound can be purified by silica gel chromatography. The times and temperatures required for complete

(32) Fields, G. B.; Noble, R. L. *Int. J. Peptide Protein Res.* **1990**, *35*, 161–214.

(33) King, D. S.; Fields, C. G.; Fields, G. B. *Int. J. Pept. Protein Res.* **1990**, *36*, 255–66.

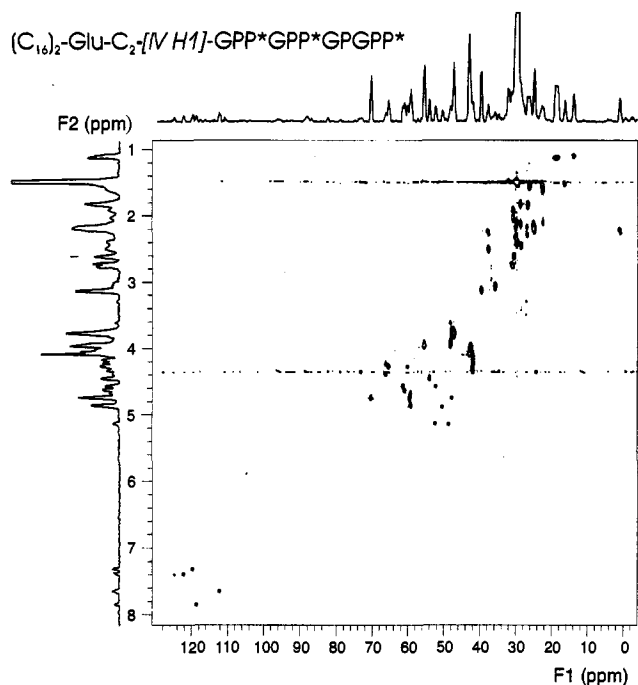


Figure 4. 500 MHz $\{^1\text{H}\}-\{^{13}\text{C}\}$ -NMR heteronuclear spin correlation (COSY) spectrum of $(\text{C}_{16})_2\text{-Glu-C}_2\text{-[IV-H1]-GPP*GPP*GPGPP*}$ amphiphile dissolved in a $\text{CD}_3\text{CN}-\text{D}_2\text{O}$ (1:1) mixture. The spectrum has been low-pass filtered, and strong solvent peaks have been eliminated with a linear prediction algorithm.

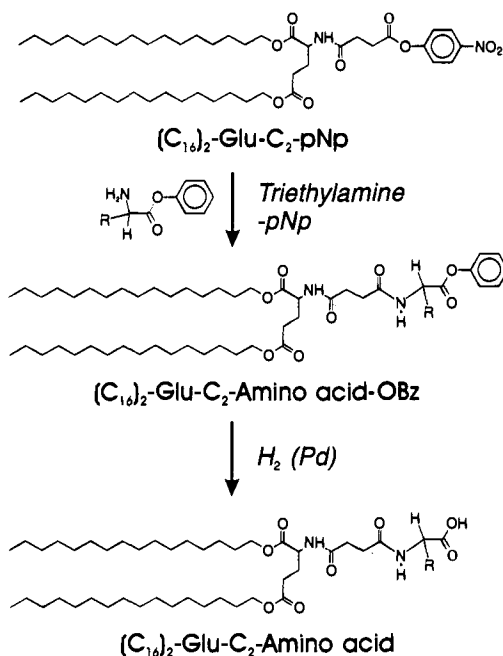


Figure 5. Liquid-phase synthesis of amino acid amphiphiles. The *p*Np-activated tail is coupled to amino acid OBz esters, and the protecting group is removed by catalytic hydrogenation.

removal of the OBz group exceeded the times given in literature for simple amino acids and peptides, which is explained by the bulkiness and hydrophobicity of the final compound. Complete removal of OBz groups from amino acid amphiphiles containing more than one protecting group (for example, $(\text{C}_{16})_2\text{-Glu-C}_2\text{-Glu(OBz)OBz}$, $(\text{C}_{16})_2\text{-Glu-C}_2\text{-Tyr(OBz)OBz}$) was found to be extremely difficult, probably due to steric hindrance or adsorption of the amphiphile on the catalyst.

Monolayer Isotherms. We investigated the behavior of monolayers of the amphiphiles at the air–water interface using pressure–area (π -A) isotherms. As expected for compounds of this chemical nature,³⁴ most amphiphile compounds formed

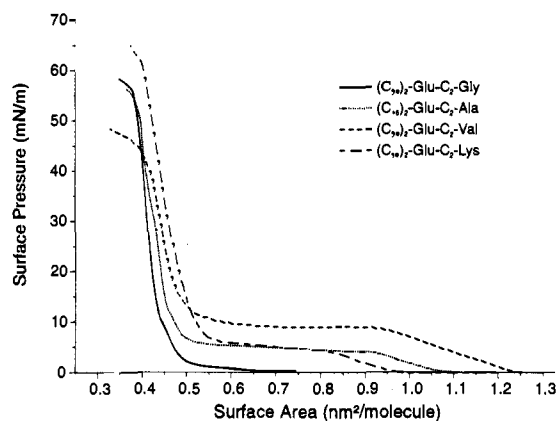


Figure 6. Surface pressure–area isotherms of amino acid amphiphiles spread over pure water at 22 °C. Whereas the glycine derivative forms only a condensed phase, increasing bulkiness and the hydrophobicity of the head group leads to the appearance of an expanded phase for the alanine and valine derivatives. The isotherm of the lysine derivative is typical for a zwitterionic compound.

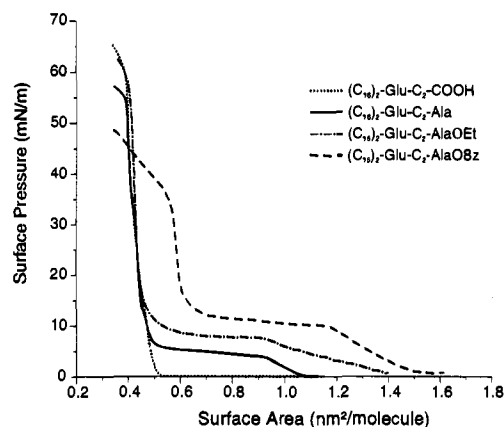


Figure 7. Surface pressure–area isotherms of ester derivatives of $(\text{C}_{16})_2\text{-Glu-C}_2\text{-Ala}$ amphiphile spread over pure water at 22 °C. Again, the appearance of an expanded phase is associated with increasing bulkiness and hydrophobicity of the head group.

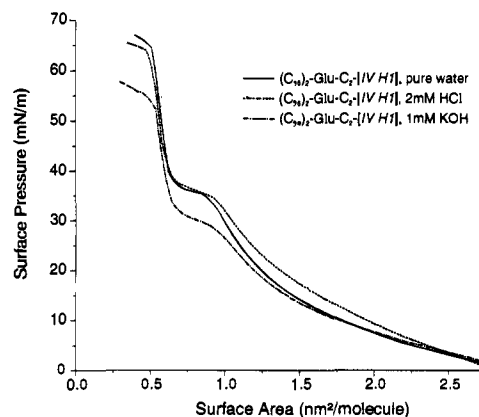


Figure 8. Surface pressure–area isotherms of $(\text{C}_{16})_2\text{-Glu-C}_2\text{-[IV-H1]}$ amphiphile spread over pure water, 2 mM HCl, and 1 mM KOH at 20 °C. The amphiphile forms an expanded phase starting at 2.5 $\text{nm}^2/\text{molecule}$ and, after a phase transition, a condensed phase at 0.58 $\text{nm}^2/\text{molecule}$. Note the different surface area scale in comparison with the figures for amino acid amphiphiles.

stable monolayers at the air–water interface with high collapse pressures in the order of 40–70 mN/m (Figures 6–9). Some of the amphiphile layers could be compressed into a condensed state as determined by a sudden rise of the surface pressure at small molecular areas.

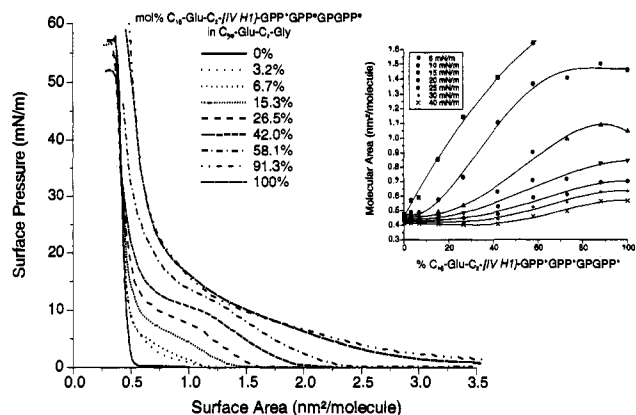


Figure 9. Mixing behavior of monolayers of $(C_{16})_2\text{-Glu-C}_2\text{-Gly}$ and $(C_{16})_2\text{-Glu-C}_2\text{-[IV-HI]-GPP*GPP*GPGPP*}$ amphiphiles spread over pure water at 22 °C. At high surface pressures, the peptide and amino acid amphiphile layers mix to form a layer that has a closer packing density than the packing density of each of the layers.

Influence of Head Group Size on Monolayer Properties.

The chemical structure of the amphiphile head group has a pronounced influence on the occurrence of an expanded phase in the measured monolayer π -A isotherm. Only the π -A isotherms of $(C_{16})_2\text{-Glu-C}_2\text{-COOH}$ (Figure 7) and $(C_{16})_2\text{-Glu-C}_2\text{-Gly}$ (Figure 6) do not show substantial rises of the surface pressure at molecular areas larger than 0.5 nm²/molecule, which is expected for uncharged or weakly charged amphiphiles with head group areas smaller or equal to the area of the tail. This molecular area corresponds to the molecular area of two long alkyl chains per molecule oriented perpendicular or slightly tilted with respect to the membrane plane.

All other investigated amphiphile monolayers feature an expanded phase, the onset of which roughly correlates with the bulkiness of the head group. However, the difference between the actual molecular areas of the head groups for, for example, glycine and alanine amphiphiles is only on the order of 0.15 nm²/molecule (the size of a single methylene group), which might cause the observed minor difference in the onset of the corresponding condensed phases (Figures 6 and 7), but cannot serve as an explanation for the occurrence of the expanded phase. Therefore, we interpret the occurrence of the expanded phase as an indication of a different head group conformation, induced by the presence of a hydrophobic side chain, instead of being brought about by an actual head group size difference. Several effects could cause this behavior: The head group could lay "on its side" (parallel to the monolayer), with the more lipophilic portion pointing or partially inserting into the tail portion. The head group portions of amphiphiles with less bulky head groups could be able to form intermolecular hydrogen bonds, thus more effectively packing the head group area in comparison to random packing for the bulkier head groups. This assumption is supported by the observation that $(C_{16})_2\text{-Glu-C}_2\text{-Gly}$ also forms a liquid expanded phase after spreading over buffered subphases with different pH (data not shown).

Noticeably, the collapse pressure of the amphiphile monolayers decreases with the bulkiness and hydrophobicity of the head group, as it is evident, for example, from the comparison of the isotherms for $(C_{16})_2\text{-Glu-C}_2\text{-Gly}$, $(C_{16})_2\text{-Glu-C}_2\text{-Ala}$, and $(C_{16})_2\text{-Glu-C}_2\text{-Val}$ (Figure 6) or from comparing the isotherms for $(C_{16})_2\text{-Glu-C}_2\text{-Ala}$, $(C_{16})_2\text{-Glu-C}_2\text{-AlaOEt}$, and $(C_{16})_2\text{-Glu-C}_2\text{-AlaOBz}$ (Figure 7). The latter monolayer cannot be compressed into a condensed state. The highest collapse pressure of about 70 mN/m was observed for $(C_{16})_2\text{-Glu-C}_2\text{-Lys}$ (Figure 6), which features a rather expanded monolayer isotherm, which, however, due to the zwitterionic nature of its

Table 1. Transfer Ratios for Langmuir-Blodgett Transfer of $(C_{16})_2\text{-Glu-C}_2\text{-[IV-HI]}$ Amphiphile from a Monolayer Spread over Pure Water to Mica

surface pressure	15 mN/m	35 mN/m	50 mN/m
up 1	1.04	1.17	1.111
down 1	0.213	0.7	0.775
up 2	0.934	1.14	1.064
down 2	-0.77	-0.81	0.779
up 3	0.952	1.15	0.94
down 3	-0.953	-0.76	N/D ^a

^a Not determined.

head group cannot be compared directly to the isotherms of amphiphiles with a single ionizable group.

We would like to emphasize that monolayer isotherms of the amphiphiles presented here show a considerable sensitivity to the hydrophobicity and size of the amino acid side chain in their head group. Further investigation of these monolayers will give us valuable information about the characteristics of amino acid side chain interaction in general.

Influence of Peptide Head Group Structure on Monolayer Properties. Peptide amphiphiles are as capable as amino acid amphiphiles of forming stable monolayers when spread over appropriate subphases. Considering the sensitivity of the measured π -A isotherms for amino acid amphiphiles on the head group structure, it comes at no surprise that the amino acid sequence of the head group has a major influence on the stability of the monolayer and the shape of the π -A isotherm.

Thus, $(C_{16})_2\text{-Glu-C}_2\text{-[IV-HI]}$, which contains 15 amino acids, gives rise to a monolayer with a large expanded phase detectable at 2.5 nm²/molecule that undergoes a noticeable transition at 1.00 nm²/molecule and can be compressed into a condensed phase at surface pressures larger than 40 mN/m and surface areas of about 0.6 nm²/molecule (Figure 8), before it collapses above 60 mN/m. When spread over different subphases, the expanded phase is slightly variable (indicating different charge/hydration states); however, the position of the phase transition is preserved. Monolayers of $(C_{16})_2\text{-Glu-C}_2\text{-[IV-HI]}$ can be transferred to substrates like mica or glass with transfer ratios of about 1.0 (Table 1). Interestingly, transfer of multilayers is possible only at very high surface pressures, above the pressure necessary for the phase transition at 1.00 nm²/molecule.

The 26-amino acid amphiphile $(C_{16})_2\text{-Glu-C}_2\text{-[IV-HI]-GPP*GPP*GPGPP*}$, in which hydrophobicity is more evenly balanced along the peptide chain, shows a simpler π -A isotherm consisting of a single expanded phase that is observed starting from a molecular area of 3.5 nm²/molecule and rises up to a limit of 0.6 nm²/molecule before the monolayer collapses at a surface pressure of 60 mN/m (Figure 9).

If we were to imagine the 15-amino acid $[IV-HI]$ peptide to be in a fully hydrated random coil configuration, we can estimate the average distance between the N and C termini to be about 1.2 nm, which would give a molecular area of at least 4.5 nm²/molecule. On the other hand, a fully dehydrated, closely packed, and fully stretched peptide chain would occupy only 0.58–0.62 nm²/molecule (assuming partial specific volumes in the range 0.68–0.75 cm³/g), with the lower extreme that of a collagen-type structure assuming one of the most dense packings possible. Finally, a globular random structure with the packing density and hydration of a "normal" protein would occupy a molecular area of 2.6–2.9 nm²/molecule. The onset of head group/head group interaction for $(C_{16})_2\text{-Glu-C}_2\text{-[IV-HI]}$ amphiphiles can be observed for molecular areas at about 2.5–3 nm²/molecule, which clearly indicates strong interaction between peptide head groups and low hydration in the monolayer even at low surface pressures. It appears also, that the exclusion limit for the monolayer (0.6 nm²/molecule) corresponds to a fully stretched,

dehydrated peptide chain. Similar conclusions can be drawn for the 26-amino acid [IV-HI]-GPP*GPP*GPGPP* peptide.

We would speculate, that the peculiar phase transition observed for $(C_{16})_2$ -Glu- C_2 -[IV-HI] amphiphile at molecular areas of 1 nm²/molecule reflects a structural transition and/or a dehydration process caused by the uneven distribution of hydrophobic residues along the peptide sequence; however, more experiments are needed to fully understand this phenomenon. Isolated [IV-HI] peptide has been shown to form stable solution structures in the NMR time scale.³⁵ Even though the sequence has been found in a triple-helical type IV collagen region, when removed from the triple-helical environment, it appears to have a considerable β -sheet-forming potential. However, when surrounded by Gly-Pro-Hyp repeats, the peptide spontaneously forms triple-helical arrangements.³¹ Upcoming NMR and FTIR investigations of densely packed LB films of this amphiphile will show whether monolayers of [IV-HI] derivatives indeed contain intermolecular hydrogen bonds characteristic for the mentioned structures.

Miscibility. In order to evaluate the biological properties of the newly synthesized peptide amphiphiles, it is useful to create membranes that mimic the density of the natural occurrence of the ligand in the extracellular matrix. Whereas it has been complicated to control the ligand density in traditional cell adhesion assays, it appears straightforward to achieve fine control over the ligand distribution in our monolayer membrane system.

Figure 9 shows π -A isotherms obtained for various mixtures of $(C_{16})_2$ -Glu- C_2 -Gly and $(C_{16})_2$ -Glu- C_2 -[IV-HI]-GPP*GPP*GPGPP* as well as a chart of the dependence of the molecular area on the molar proportion of peptide amphiphile in the mixture for various given surface pressures. From these data it can be seen that the resulting isotherm for a mixture of peptide and amino acid amphiphiles is different from the weighted sum of the individual isotherms. This appears especially striking at high surface pressures, where up to one-half of the amino acid amphiphile can be replaced with peptide amphiphile without any change in surface pressure. This clearly indicates molecular mixing of both amphiphiles. On the other hand, this effect cannot be observed at lower surface pressures, where therefore separate amino acid and peptide amphiphile domains exist. A small addition of amino acid amphiphile to a peptide monolayer actually leads to a considerable expansion of the layer, indicating disordering and diminished packing density of the peptide head groups induced by the "holes" in the head group region created by the small amino acid amphiphile.

[HEP III]-Derived Amphiphile. In contrast to above-mentioned [IV-HI]-derived amphiphiles, $(C_{16})_2$ -Glu- C_2 -[HEP III] amphiphile does not form well-defined monolayers when spread over pure water (Figure 10). The layers formed by this amphiphile are unstable (the obtained isotherm is dependent on the compression speed, and the surface area decreases with time when held at constant surface pressure). Furthermore, the surface pressure rises only at extremely small surface areas. This behavior is similar to that of long-chain hydrocarbons, and it is rationalized considering the hydrophobicity of the amino acid sequence and assuming that the four ionizable groups form intramolecular salt bridges. The increased charge of the head group that is obtained when the amphiphile is spread over 2 mM HCl stabilizes the monolayer. Over an acidic subphase a positive surface pressure can be detected at molecular areas of 1.0 nm²/molecule; however, the low collapse pressure of 30

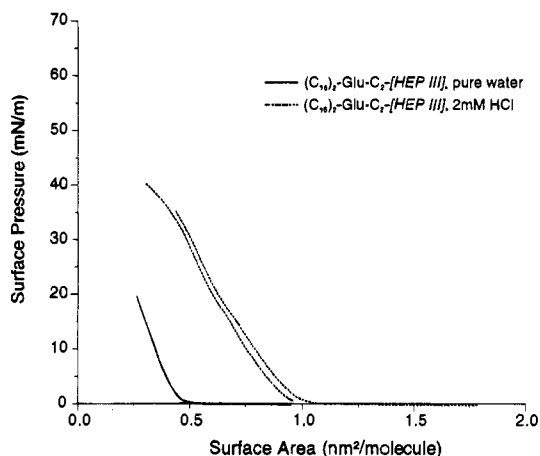


Figure 10. Surface pressure–area isotherms of $(C_{16})_2$ -Glu- C_2 -[HEP III] amphiphile spread over pure water and 2 mM HCl at 20 °C. This amphiphile does not form stable monolayers when spread over pure water, which is probably due to the hydrophobicity of the head group and the formation of intramolecular salt bridges for the polar residues in the sequence. When the amphiphile obtains a net charge (e.g., due to the presence of strong acid in the subphase), monolayer behavior is noticeably improved.

mN/m still leaves this monolayer short of the excellent stability observed for $(C_{16})_2$ -Glu- C_2 -[IV-HI].

Conclusion

We have synthesized a variety of amphiphiles with different amino acid- or peptide-containing head groups using a simple, general, and highly efficient approach. Most of these amphiphiles are capable of forming stable monolayers at the air–water interface and can be transferred to different solid substrates using conventional Langmuir–Blodgett technique. Monolayer studies give interesting insights into the details of amino acid side chain and peptide–peptide interactions. In addition, preliminary data (not shown) indicates that amino acid amphiphiles are capable of forming bilayer membranes and vesicles. Therefore, we have obtained a useful tool for orienting, assembling, and stabilizing peptide structures and studying their interaction with other cellular or soluble ligands. Layers containing similar amphiphiles could have important practical applications as targeting agents in drug delivery systems or as bioaffinity coatings.

Experimental Section

Materials and Reagents. GlyOBz was synthesized as described by Bodanszky *et al.*;³⁶ AlaOBz, Lys(Z)-OBz, and Val-OBz were obtained from BACHEM Bioscience Inc. Fmoc-amino acids used for peptide synthesis were from Milipore Corp. Triethylamine was redistilled from phthalic anhydride and KOH. Ultrapure water with a resistance of more than 18.2 M Ω /cm was obtained with a Milli-Q UV-Plus system. All other reagents and solvents were at least analytical grade and used as supplied.

General Methods. NMR spectra were measured with Bruker AC200 or Varian 500 spectrophotometers; FTIR spectra were recorded with a Nicolet instrument on KBr pellets. Low-resolution FAB or ES-mass spectra were registered using a VG 7070E-HF instrument with an accelerating voltage of 5 kV and Xenon as reagent gas. Scans were made using glycerol:TFA and MNBA:TFA matrices. Peptide amphiphiles were analysed by time-of-flight mass spectroscopy (positive polarity, linear flight path) using a Kratos Kompact MALDI I system with samples dissolved in 10% acetonitrile:0.1% trifluoroacetic acid and evaporized from sinapinic acid (analysis courtesy of Shimadzu Scientific). Melting points were measured by differential scanning calorimetry using a Perkin-Elmer DSC-7 at scan rates between 5 and 40 °C/min or a conventional Electrothermal 9200 melting point apparatus. Melting points are uncorrected. HPLC was carried out on

(35) Mayo, K. H.; Parra-Diaz, D.; McCarthy, J. B.; Chelberg, M. *Biochemistry* **1991**, *30*, 8251–67.

(36) Bodanszky, M.; Bodanszky, A. *The practice of peptide synthesis*; Springer: Heidelberg, Germany, 1984; p 42.

a Shimadzu LC10A dual-pump system equipped with a PDA 10 photodiode array detector. Monolayer isotherms were measured using a fully computerized KSV LB5000 Langmuir-Blodgett trough with a platinum Wilhelmi plate as sensor. Amphiphiles were spread from chloroform(4):hexane(5):methanol(1) solutions. Barrier movement was initiated 5–15 min after spreading. Isotherms were acquired with the barrier moving at constant speeds in the range from 2 to 50 mm/min. If not otherwise stated, no dependence of the shape of the isotherm on spreading conditions or on the speed of the barrier movement was observed.

Organic Synthesis. 1',3'-Dihexadecyl L-Glutamate (pTs Salt). The procedure is based on the protocol given by Asakuma.²⁵ Hexadecanol (44.85 g, 0.185 mol) and Glu (13.6 g, 0.092 mol) were mixed with 21.0 g (0.102 mol) of *p*-toluenesulfonate in toluene, and the mixture was heated until an equimolar amount of water was recovered in a Dean-Stark trap. The toluene was removed, and the product recrystallized from acetone. Yield: 80%. TLC (silica gel K60) methanol (1):chloroform (99): R_f 0.3 (pTs salt); R_f 0.05 (free amine). ¹H-NMR: δ_{CDCl_3} 0.87 (t, 6, -CH₃), 1.25 (m, >50, -CH₂-), 1.53 (m, 4, -CH₂-CH₂-OCO), 2.19 (tt, 2, -COCH₂CH₂CHCO,NH), 2.34 (s, 3, -C₆H₄CH₃), 2.45 (h, 2, -COCH₂CH₂-), 4.00 (tt, 4, -CH₂OCO-), 7.76, 7.72, 7.14, 7.10 (dd, 4, -OSO₃C₆H₄CH₃), 8.29 (b, 2-3, -NH₃⁺-OSO₃⁻). FTIR: NH₂ val (3400 cm⁻¹, 1510 cm⁻¹), aryl CH₂ (3050 cm⁻¹), CH₃ val assym (2954 cm⁻¹), CH₂ val assym (2917 cm⁻¹), CH₃ val sym (2893 cm⁻¹), CH₂ val sym (2850 cm⁻¹), amine salt (broad >2800 cm⁻¹), ester CO val (1760 cm⁻¹), aromatic ring (1580, 1500, 1450 cm⁻¹).

1',3'-Dihexadecyl N-Succinyl-L-glutamate. 1',3'-Dihexadecyl L-glutamate (20 g, 26 mmol) and triethylamine (5.5 mL, 39 mmol) were dissolved in a 1:1 THF:CHCl₃ mixture, and 3.9 g (39 mmol) of succinic anhydride was added under stirring. The mixture was kept for 4 h at 30 °C. The product obtained after removal of the solvent was recrystallized from acetone and ethanol.

Yield: 94%. Mp: 74.5 °C. TLC (silica gel K60) chloroform/methanol (96:4): R_f 0.4. ¹H-NMR: δ_{CDCl_3} 0.87 (t, 6H, -CH₃), 1.25 (m, >50, CH₂), 1.53 (m, 4, -CH₂CH₂OCO), 1.91, 2.09 (tt, 2, -COCH₂CH₂CHCO,NH), 2.25 (h, 2, -COCH₂CH₂CHCO,NH), 2.35, 2.45 (tt, 4, NHCOCH₂CH₂COOH), 4.00 (tt, 4, -CH₂OCO), 4.59 (tt, 1, CH₂CHCO,NH), 6.56 (d, 1, OCOCHNHCO-). FAB-MS: 696.6 (MH⁺), 694.6 (M⁻); FTIR: OH val (3510 cm⁻¹), CH₃ val assym (2954 cm⁻¹), CH₂ val assym (2917 cm⁻¹), CH₃ val sym (2893 cm⁻¹), CH₂ val sym (2850 cm⁻¹), ester carbonyl (1780 cm⁻¹), acid CO (1730 cm⁻¹), amide CO val (1640 cm⁻¹), amide NH (1540 cm⁻¹).

1',3'-Dihexadecyl N-[O-(4-Nitrophenyl)succinyl]-L-glutamate. 1',3'-Dihexadecyl N-succinyl-L-glutamate (6.90 g, 9.9 mmol) and *p*-nitrophenol (1.65 g, 11.9 mmol) were dissolved in CH₂Cl₂ and 2.05 g (9.9 mmol) of *N,N*-dicyclohexylcarbodiimide as well as a catalytic amount (80 mg) of (dimethylamino)pyridine was added to the reaction mixture on an ice bath. The reaction was continued for 2 h on the ice bath and for 24 h at room temperature. The formed dicyclohexylurea was filtered off, and the reaction product was precipitated with cold dry ethanol. Yield: 85%. Mp: 89 °C. TLC (silica gel K60) methanol (5):chloroform (95): R_f 0.7. ¹H-NMR: δ_{CDCl_3} 0.87 (t, 6H, -CH₃), 1.25 (m, >50, -CH₂-), 1.53 (m, 4, -CH₂CH₂OCO), 1.91, 2.09 (tt, 2, -COCH₂CH₂CHCO,NH), 2.25 (h, 2, -COCH₂CH₂CHCO,NH), 2.35, 2.45 (tt, 4, NHCOCH₂CH₂COOH), 4.00 (tt, 4, -CH₂OCO-), 4.59 (tt, 1, CH₂CHCO,NH), 6.56 (d, 1, OCOCHNHCO-), 7.29, 7.25 (d, 2, -COOC₆H₄NO₂), 8.36, 8.31 (d, 2, -COOC₆H₄NO₂).

1',3'-Dihexadecyl N-[1-(*N*-Aminoacyl-*O*-benzoyl ester)succinyl]-L-glutamates. The *p*-toluenesulfonate salt³⁷ (6.5 mmol) of the appropriate OBz-protected amino acid was suspended in 100 mL of ethyl acetate. After addition of 2.7 mL (19.5 mmol) of triethylamine, the solution became clear. 5 g (6.2 mmol) of 1',3'-Dihexadecyl N-[O-(4-nitrophenyl)succinyl]-L-glutamate (5 g, 6.2 mmol) was dissolved in ethyl acetate and added to the reaction mixture. The solution was stirred for at least 24 h at room temperature. Thereafter, the solvent was evaporated and the residue was dried under vacuum. The product was purified by recrystallization from absolute ethanol. The reaction yields range from 66% (C₁₆-glu-C₂-Lys(Z)-OBz) to 97% (C₁₆-glu-C₂-GlyOBz).

1',3'-Dihexadecyl N-[1-(*N*-Glycyl-*O*-benzoyl ester)succinyl]-L-glutamate. Yield: 97%. Mp: 88.9 °C. TLC (silica gel K60) methanol (10):chloroform (90): R_f 0.85. ¹H-NMR: δ_{CDCl_3} 0.87 (t, 6, -CH₃),

1.25 (m, >50, -CH₂-), 1.59 (m, 4, -CH₂CH₂OCO), 1.91, 2.09 (tt, 1+1, -COCH₂CH₂CHCO,NH), 2.35 (h, 2, -COCH₂CH₂CHCO,NH), 2.57 (t, 4, NHCOCH₂CH₂CONH), 4.03 (s, 2, NHCH₂COOBz), 4.05 (tt, 4, -CH₂OCO-), 4.55 (tt, 1, CH₂CHCO,NH), 5.16 (s, 2, CH₂-COOCH₂C₆H₅), 6.54 (d, 2, -NHCO-), 7.34 (s, 5, CH₂COOCH₂C₆H₅). ¹³C-NMR: $\delta_{\text{CDCl}_3, \text{CD}_3\text{OD}}$ 13.7 (CH₃CH₂-), 22.5 (CH₃CH₂-), 29.2 (alkyl-CH₂-), 31.75 (CH₃CH₂CH₂-), 40.9 (-NHCH₂COOBz), 51.7 (-OCCH₂CH₂CHCO(NH)-), 57.4 (-OCCH₂CH₂CHCO(NH)-), 64.9, 65.6 (COOCH₂CH₂-), 66.9 (COOCH₂C₆H₅), 128.3 (-CH₂C₆H₅, C₄), 128.4 (-CH₂C₆H₅, C_{2,3,5,6}), 135.1 (CH₂C₆H₅, C₁), 172.0, 172.9, 173.1 (-COOR). FAB-MS: [M + H]⁺ 843.7, [M + Na]⁺ 865.6, FB⁺ fragments: 596.6, 678.6, no FB⁻ fragments.

1',3'-Dihexadecyl N-[1-(*N*-Alanyl-*O*-benzoyl ester)succinyl]-L-glutamate. Yield: 85%. Mp: 97.4 °C. TLC (silica gel K60) methanol (10):chloroform (90): R_f 0.9. ¹H-NMR: δ_{CDCl_3} 0.88 (t, 6, -CH₃), 1.25 (m, >50, -CH₂-), 1.38, 1.41 (d, 3, -NHCH(CH₃)COOBz), 1.57 (m, 4, -CH₂CH₂OCO), 1.95, 2.10 (tt, 1+1, -COCH₂CH₂CHCO,NH), 2.36 (h, 2, -COCH₂CH₂CHCO,NH), 2.54 (t, 4, NHCOCH₂CH₂CONH), 4.05 (tt, 4, -CH₂OCO-), 4.55 (t, 1, CH₂CHCO,NH), 5.15 (s, 2, CH₂-COOCH₂C₆H₅), 6.54 (m, <2, -NHCO-), 6.62 (d, 1, -CH₂CH₂-CONHCH(CH₃)-), 7.34 (s, 5, CH₂COOCH₂C₆H₅). ¹³C-NMR: $\delta_{\text{CDCl}_3, \text{CD}_3\text{OD}}$ 13.7 (CH₃CH(NH)COOBz), 13.8 (CH₃CH₂-), 22.5 (CH₃CH₂-), 29.2 (alkyl-CH₂-), 31.75 (CH₃CH₂CH₂-), 39.5 (weak, -NHCH(CH₃)COOBz), 51.7 (-OCCH₂CH₂CHCO(NH)-), 57.4 (-OCCH₂CH₂CHCO(NH)-), 64.9, 65.6 (COOCH₂CH₂-), 66.9 (COOCH₂C₆H₅), 128.3 (-CH₂C₆H₅, C₄), 128.4 (-CH₂C₆H₅, C_{2,3,5,6}), 135.1 (CH₂C₆H₅, C₁), 172.0, 172.9, 173.1 (-COOR). FAB-MS: [M + H]⁺ 857.6, [M + Na]⁺ 879.6, [M - H]⁻ 855.6, FB⁺ fragments: 596.5, 678.5, FB⁻ fragment: 765.6.

1',3'-Dihexadecyl N-[1-(*N*-Valinyl-*O*-benzoyl ester)succinyl]-L-glutamate. Yield: 97%. Mp: 93.2 °C. TLC (silica gel K60) methanol (10):chloroform (90): R_f 0.85. ¹H-NMR: δ_{CDCl_3} 0.86 (t, 12, -CH₃), 1.24 (m, >50, -CH₂-), 1.69 (m, 4, -CH₂CH₂OCO-), 1.95 (m, 1, -CHCH(CH₃)₂), 2.09 (tt, 1 + 1, -COCH₂CH₂CHCO,NH), 2.35 (h, 2, -COCH₂CH₂CHCO,NH), 2.56 (t, 4, NHCOCH₂CH₂CONH), 4.07 (tt, 4, -CH₂OCO-), 4.48 (m, 2, NHCHCO), 5.13 (d, 2, CH₂COOCH₂C₆H₅), 6.44, 6.58 (dd, 1 + 1, -NHCO-, not present after addition of CD₃-OD), 7.34 (s, 5, CH₂COOCH₂C₆H₅). ¹³C-NMR: $\delta_{\text{CDCl}_3, \text{CD}_3\text{OD}}$ 13.7 (CH₃-CH₂-), 17.6, 18.8 CH(CH₃)₂, 22.5 (CH₃CH₂-), 29.2 (alkyl-CH₂-), 31.75 (CH₃CH₂CH₂-), 38.5 (weak, -NHCHCOOH), 51.7 (-OCCH₂CH₂CHCO(NH)-), 57.4 (-OCCH₂CH₂CHCO(NH)-), 64.9, 65.6 (COOCH₂CH₂-), 66.9 (COOCH₂C₆H₅), 128.3 (-CH₂C₆H₅, C₄), 128.4 (-CH₂C₆H₅, C_{2,3,5,6}), 135.1 (CH₂C₆H₅, C₁), 172.0, 172.9, 173.1 (-COOR). FAB-MS: [M + H]⁺ 885.7, [M + Na]⁺ 907.7, [M - H]⁻ 883.7, FB⁺ fragments: 596.6, 678.6, no FB⁻ fragments.

1',3'-Dihexadecyl N-[1-(*N*-[ε-*N*-Carboxybenzoyl]-lysyl-*O*-benzoyl ester)succinyl]-L-glutamate. Yield: 66%. Mp: 97.2 °C. TLC (silica gel K60) methanol (10):chloroform (90): R_f 0.5. ¹H-NMR: δ_{CDCl_3} 0.86 (t, 6, -CH₃), 1.25 (m, 60, CH₂), 1.40 (b, 2, -CH₂CH₂CH₂NH₂), 1.57 (m, 4, -CH₂CH₂OCO), 1.7 (b, >3, -CH₂CH₂CH₂CH₂NH₂), 1.95, 2.15 (tt, 1 + 1, -COCH₂CH₂CHCO,NH), 2.33 (h, 2, -COCH₂CH₂CHCO,NH), 2.52 (t, 4, NHCOCH₂CH₂CONH), 3.01 (t, 2, -CH₂CH₂CH₂CH₂-NH₂), 4.05 (tt, 4, -CH₂OCO-), 4.56 (tt, 1, CH₂CHCO,NH), 5.07 (s, 2, CH₂COOCH₂C₆H₅), 5.12, 5.14 (d, 2, -CH₂NHCOOCH₂C₆H₅), 6.67 (d, >1, -NHCO-), 7.32 (s, 10, -CH₂C₆H₅). ¹³C-NMR: δ_{CDCl_3} 14.1 (CH₃CH₂-), 22.7 (CH₃CH₂-), 29.7 (alkyl-CH₂-), 31.9 (CH₃CH₂-CH₂-), 52.4 (-OCCH₂CH₂CHCO(NH)-), 58.2 (-OCCH₂CH₂CHCO(NH)-), 64.9, 65.4 (COOCH₂CH₂-), 66.9, 67.4 (COOCH₂C₆H₅), 128.5 (-CH₂C₆H₅), numerous peaks, not resolved, 173.1, 173.7 (-COOR). FAB-MS: [M + H]⁺ 1048.8, [M + Na]⁺ 1070.8, FB⁺ fragments: 596.6, 678.6, 914.7, FB⁻ fragment: 956.9.

1',3'-Dihexadecyl N-[1-(*N*-Aminoacyl)succinyl]-L-glutamates. (4 g, 5 mmol) 1',3'-Dihexadecyl N-[1-(*N*-aminoacyl-*O*-benzoyl ester)succinyl]-L-glutamate was dissolved in chloroform.³⁸ Palladium catalyst on charcoal³⁹ (0.4 g) was added, and the mixture was flushed with nitrogen gas. Thereafter the introduction of a slow stream of hydrogen was started. The catalyst was kept in suspension with vigorous stirring.

(38) A small amount of ethanol was added to facilitate dissolution of the compound. However, we could identify one of the byproducts of the reaction as the ethyl ester of the goal compound. Therefore, treatment with alcohol should be avoided.

(39) Washed with chloroform/methanol (3:1) and filtered through a coarse sinter filter.

The reaction was continued for 6 h at 35 °C. Thereafter, the hydrogen gas was replaced by nitrogen and the stirring was stopped. The reaction mixture was filtered through a fine glass filter, and the solvent was removed under vacuum. The reaction product was recrystallized from ethanol and purified by chromatography on silica gel K60. The compounds were applied to a 20 × 1.5 cm column in hexane/CHCl₃/methanol (50:49:1), washed with 300 mL of this solvent mixture, and eluted with hexane/CHCl₃/methanol (5:4:1).⁴⁰ Elution was followed by HPTLC on silica gel with phosphomolybdate in ethanol as detecting agent. We identified (C₁₆)₂-glu-C₂-aminoacyl-OEt and unreacted (C₁₆)₂-glu-C₂-aminoacyl-OBz as two minor impurities that were separated during the chromatographic procedure. Yields (before chromatography) were in the range between 77% ((C₁₆)₂-glu-C₂-Gly) and 92% ((C₁₆)₂-glu-C₂-Ala).

1',3'-Dihexadecyl N-[1-(N-Glycyl)succinyl]-L-glutamate. Yield: 77%. Mp: 85.4 °C. TLC (silica gel K60) methanol (1):chloroform (9): *R_f* 0.15. ¹H-NMR: δ_{CDCl₃, CD₃OD} 0.87 (t, 6H, -CH₃), 1.25 (m, >50, CH₂), 1.59 (m, 8, -CH₂CH₂OCO), 1.91, 2.09 (tt, 1+1, -COCH₂CH₂CHCO, NH), 2.35 (h, 2, COCH₂CH₂CHCO, NH), 2.57 (t, 4, NHCOCH₂CH₂-CONH), 3.77 (d, 2, NHCH₂COOH), 4.05 (tt, 4, -CH₂OCO-), 4.35 (tt, 1, CH₂CHCO, NH). ¹³C-NMR δ_{CDCl₃, CD₃OD} 13.7 (CH₃CH₂-), 22.5 (CH₃CH₂-), 29.2 (alkyl-CH₂-), 31.75 (CH₃CH₂CH₂-), 40.9 (-NHCH₂COOH), 51.7 (-OCCH₂CH₂CHCO(NH)-), 57.4 (-OCCH₂CH₂CHCO(NH)-), 64.9, 65.6 (COOCH₂CH₂-), 172.0, 171.9, 173.0 (-COOH, -COOR). FAB-MS: [M + H]⁺ 753.6, [M + Na]⁺ 775.6, [M + K]⁺ 791.6, [M - H]⁻ 751.6, FB⁺ fragments: 596.6, 678.6. FTIR: amide NH val (3301 cm⁻¹), COOH OH val (3070 cm⁻¹), CH₃ val assym (2954 cm⁻¹), CH₂ val assym (2917 cm⁻¹), CH₃ val sym (2893 cm⁻¹), CH₂ val sym (2850 cm⁻¹), ester CO val (1739 cm⁻¹), amide CO val (1644 cm⁻¹), amide NH (1536 cm⁻¹), CH₃ assym def, CH₂ scissor (1467 cm⁻¹), CH₃ sym def ((w) 1379 cm⁻¹).

1',3'-Dihexadecyl N-[1-(N-Alanyl)succinyl]-L-glutamate. Yield: 92%. Mp: 86.7 °C. TLC (silica gel K60) methanol (1):chloroform (9): *R_f* 0.10. ¹H-NMR: δ_{CDCl₃, CD₃OD} 0.72 (t, 6, -CH₃), 1.10 (m, >50, -CH₂-), 1.21, 1.26 (d, 3, -NHCH(CH₃)COOH), 1.46 (m, 4, -CH₂-CH₂OCO), 1.87, 2.05 (tt, 1+1, -COCH₂CH₂CHCO, NH), 2.24 (h, 2, -COCH₂CH₂CHCO, NH), 2.38 (t, 4, NHCOCH₂CH₂-CONH), 4.01 (tt, 4, -CH₂OCO-), 4.35 (tt, 1, CH₂CHCO, NH). ¹³C-NMR: δ_{CDCl₃, CD₃OD} 13.7 (CH₃CH(NH)COOH), 13.8 (CH₃CH₂-), 22.5 (CH₃CH₂-), 29.2 (alkyl-CH₂-), 31.75 (CH₃CH₂CH₂-), 39.5 (weak, -NHCH(CH₃)COOBz), 51.7 (-OCCH₂CH₂CHCO(NH)-), 57.4 (-OCCH₂CH₂CHCO(NH)-), 64.9, 65.6 (COOCH₂CH₂-) 171.5, 172.9, 173.1 (-COOH, -COOR). FAB-MS: [M + K]⁺ 805.5, [M - H]⁻ 765.7, FB⁺ fragments: 583.3, 678.5. FTIR: amide NH val (3310 cm⁻¹), COOH OH val (3100 cm⁻¹), CH₃ val assym (2958 cm⁻¹), CH₂ val assym (2920 cm⁻¹), CH₃ val sym (2880 cm⁻¹), CH₂ val sym (2855 cm⁻¹), ester CO val (1742 cm⁻¹), amide CO val (1642 cm⁻¹), amide NH (1540 cm⁻¹), CH₃ assym def, CH₂ scissor (1460 cm⁻¹), CH₃ sym def ((w) 1380 cm⁻¹).

1',3'-Dihexadecyl N-[1-(N-Alanyl-O-ethyl ester)succinyl]-L-glutamate. This compound was isolated as minor fraction during purification of (C₁₆)₂-glu-C₂-Ala and identified by NMR and FAB-MS. Mp: 87.5 °C. TLC (silica gel K60) methanol (1):chloroform (9) *R_f* 0.35; δ_{CDCl₃} 0.82 (t, 6, -CH₃), 1.26 (m, >50, -CH₂-), 1.31, 1.34 (d, 3, -NHCH(CH₃)COOH), 1.58 (m, 4, -CH₂CH₂OCO), 1.87, 2.05 (tt, 1+1, -COCH₂CH₂CHCO, NH), 2.24 (h, 2, -COCH₂CH₂CHCO, NH), 2.38 (t, 4, NHCOCH₂CH₂-CONH), 4.01 (tt, 4, -CH₂OCO-), 4.19, 4.22 (q, 2, -CO(O)CH₂CH₃), 4.35 (tt, 1, CH₂CHCO, NH), 6.59, 6.75 (-NHCO-); FAB-MS [M + H]⁺ 795.6, [M + Na]⁺ 817.7.

1',3'-Dihexadecyl N-[1-(N-Valinyl)succinyl]-L-glutamate. Yield: 83%. Mp: 75.4 °C. TLC (silica gel K60) hexane (50):chloroform (42):methanol (8): *R_f* 0.25. ¹H-NMR (600 MHz): δ_{CDCl₃} 0.87 (t, 6, -CH₃), 0.96 (t, 6, -CH(CH₃)₂), 1.24 (m, >50, -CH₂-), 1.61 (m, 4, -CH₂-CH₂OCO-), 2.00 (m, 1, -NHCH(CH₃)₂), 2.18 (m, 1 + 1, -COCH₂CH₂-CHCO, NH), 2.36 (m, 2, -COCH₂CH₂CHCO, NH), 2.65 (s, 4, NHCOCH₂CH₂-CONH), 4.05, 4.12 (tt, 4, -CH₂OCO-), 4.48, 4.56 (m, 1 + 1, NHCHCO), 7.05 (m, 2, -NHCO-). ¹³C-NMR: δ_{CDCl₃, CD₃OD} 13.9 (CH₂H₂-), 17.5, 18.8 (CH(CH₃)₂), 22.6 (CH₃CH₂-), 29.2 (alkyl-CH₂-), 31.8 (CH₃CH₂CH₂-), 51.7 (-OCCH₂CH₂CHCO(NH)-), 57.4 (-OCCH₂CH₂CHCO(NH)-), 65.0, 65.7, (COOCH₂CH₂-), 172.0,

173.0, 173.8 (-COOH, -COOR). FAB-MS: [M + H]⁺ 795.6, [M + Na]⁺ 817.6, [M + K]⁺ 833.5, [M - H]⁻ 793.5, FB⁺ fragments: 596.5, 678.5, no FB⁻ fragments. FTIR: amide NH val (3350 cm⁻¹), COOH OH val (3085 cm⁻¹), CH₃ val assym (2961 cm⁻¹), CH₂ val assym (2920 cm⁻¹), CH₃ val sym (2870 cm⁻¹), CH₂ val sym (2849 cm⁻¹), ester CO val (1743 cm⁻¹), amide CO val (1640 cm⁻¹), amide NH (1535 cm⁻¹), CH₃ assym def, CH₂ scissor (1466 cm⁻¹), CH₃ sym def ((w) 1375 cm⁻¹).

1',3'-Dihexadecyl N-[1-(N-Lysyl)succinyl]-L-glutamate. Yield: 89%. Mp: 135 °C. TLC (silica gel K60) hexane (50):chloroform (42):methanol (8): *R_f* 0.05. ¹H-NMR: δ_{CDCl₃, CD₃OD} 0.81 (t, 6, -CH₃), 1.18 (m, >50, CH₂), 1.54 (m, 4, -CH₂CH₂OCO), 1.91, 2.09 (tt, 1 + 1, -COCH₂CH₂CHCO, NH), 2.35 (h, 2, -COCH₂CH₂CHCO, NH), 2.57 (t, 4, NHCOCH₂CH₂-CONH), 2.89 (m, 2, -CH₂NH₂), 4.01 (tt, 4, -CH₂-OCO-), 4.18, 4.40 (tt, 1 + 1, CH₂CHCO, NH). ¹³C-NMR δ_{CDCl₃, CD₃OD} 14.2 (CH₃H₂-), 22.7 (CH₃CH₂-), 29.4 (alkyl-CH₂-), 31.9 (CH₃-CH₂CH₂-), 51.9 (-OCCH₂CH₂CHCO(NH)-), 58.0 (-OCCH₂CH₂-CHCO(NH)-), 58.6 (-CH₂NH₂), 65.1, 65.9 (COOCH₂CH₂-), 171.2, 173.0 (-COOH, -COOR). FAB-MS: [M + H]⁺ 824.7, [M + Na]⁺ 846.6, [M + K]⁺ 862.6, [M - H]⁻ 822.7, FB⁺ fragments: 596.4, 678.3, no FB⁻ fragments. FTIR: amine NH val (3350 cm⁻¹), amide NH val (2990 cm⁻¹), COOH OH val (3080 cm⁻¹), CH₃ val assym (2960 cm⁻¹), CH₂ val assym (2920 cm⁻¹), CH₃ val sym (2870 cm⁻¹), CH₂ val sym (2850 cm⁻¹), ester CO val (1740 cm⁻¹), amide CO val (1640 cm⁻¹), primary amine NH (1600 cm⁻¹), amide NH (1536 cm⁻¹), CH₃ assym def, CH₂ scissor (1467 cm⁻¹), CH₃ sym def ((w) 1379 cm⁻¹).

1',3'-Dihexadecyl N-[1-(N-Peptidyl)succinyl]-L-glutamates. *N*-Dihexadecyl *N*-[1-(*N*-peptidyl)succinyl]-*L*-glutamates were synthesized by incubation of the appropriate NH₂-peptidyl-resin (obtained after incubation of the fully protected Fmoc-peptidyl-resin for 20 min in piperidine/dimethylformamide (1:4) and washing with DMF) with a 4-fold molecular excesses of *N*-dihexadecyl *N*-[*O*-(4-nitrophenyl)succinyl]-*L*-glutamate and 1-hydroxybenzotriazole over the substitution level of the resin in a dimethylformamide:dichloromethane (1:1) mixture. The reaction was followed by the Kaiser test for free amine on the resin. After 4 h, the amphiphile was deprotected and cleaved by incubation with 95% trifluoroacetic acid in dichloromethane for peptides not containing Trp or Reagent K³³ for Trp-containing peptides. The amphiphiles were precipitated with cold ether, lyophilized, and purified by reverse phase HPCL on a Vydac C4 2.5 × 25 column using 55%–90% acetonitrile gradients or 80% acetonitrile isocratic elution.

LD-MS. (C₁₆)₂-Glu-C₂-Gly-Val-Lys-Gly-Asp-Lys-Gly-Asn-Pro-Gly-Trp-Pro-Gly-Ala-Pro-Tyr (= (C₁₆)₂-Glu-C₂-[IV-HI]): [M + H]⁺ 2277.2, calcd 2278.4; (C₁₆)₂-Glu-C₂-Gly-Val-Lys-Gly-Asp-Lys-Gly-Asn-Pro-Gly-Trp-Pro-Gly-Ala-Pro-Gly-Pro-Hyp-Gly-Pro-Hyp-Gly-Pro-Gly-Pro-Hyp (= (C₁₆)₂-Glu-C₂-[IV-HI]-GPP*GPP*GPP*): [M + H]⁺ 3068.9, calcd 3069.5.

ES-MS. (C₁₆)₂-Glu-C₂-Gly-Glu-Phe-Tyr-Phe-Asp-Leu-Arg-Leu-Lys-Gly-Asp-Lys (= (C₁₆)₂-Glu-C₂-[HEP III]): [M + H]⁺ 2430.4 Da, calcd 2430.1 Da.

Abbreviations: (C₁₆)₂-Glu-C₂-COOH, 1',3'-dihexadecyl *N*-succinyl-*L*-glutamate; (C₁₆)₂-Glu-C₂-pNp, 1',3'-dihexadecyl *N*-[*O*-(4-nitrophenyl)succinyl]-*L*-glutamate; Boc, *tert*-butyloxycarbonyl; DCCI, dicyclohexylcarbodiimide; DIPCI, diisopropylcarbodiimide; DMAP, (dimethylamino)pyridine; DMF, dimethylformamide; Fmoc, 9-fluorenylmethoxycarbonyl; HOBt, hydroxybenzotriazole; HPLC, high-performance liquid chromatography; OBz, benzoyl; pNp, *p*-nitrophenyl; pTs, *p*-toluenesulfonate; Z, carboxybenzoyl; OEt, ethyl; TEA, triethanolamine.

Acknowledgment. We thank C. Fields and Y. C. Yu for their help in the synthesis of some of the peptide amphiphiles, S. Kumar for DSC analysis, and R. Davis for his helpful advice in 2D-NMR experiments. Peptide amphiphile mass spectrometric analysis was conducted by Dr. Ayukawa (Shimadzu Scientific). This work has been supported in part by the Center for Interfacial Engineering, an NSF Engineering Research Center at the University of Minnesota, and by the Earl E. Bakken Chair in Biomedical Engineering.

(40) (C₁₆)₂-Glu-C₂-Lys was eluted with hexane/chloroform/methanol/water (20:16:3:1) and monitored by reaction of the lysine side chain amine with ninhydrine.